Indian Journal of Chemical Technology
Vol. 29, September 2022, pp. 473-484
DOI: 10.56042/ijct.v29i5.62741

Kinetics and *in vitro* release studies of drug loaded silver nanoparticles from *Indigofera tinctoria* extract

Yasmin Khambhaty*[,1], Suryakiran Bondada[1] & Sujata Mandal[2]

[1]Microbiology Division, CSIR-Central Leather Research Institute, Adyar, Chennai 600 020, India

[2]Centre for Analysis, Testing, Evaluation & Reporting Services (CATERS) CSIR-Central Leather Research Institute, Adyar, Chennai 600 020, India

E-mail: yasmink@clri.res.in

Received 27 April 2022; accepted 4 August 2022

Silver nanoparticles (AgNP's) have been successfully fabricated via bio-reduction of *Indigofera tinctoria* plant extract as the reducing and capping agent. The effects of *p*H and temperature on the formation of the AgNP's have been studied. The synthesized AgNP's have been characterized using UV-Visible spectroscopy, Fourier Transform Infrared (FTIR) spectroscopy, Zeta potential analysis, Scanning Electron Microscope (SEM) and Atomic Force Microscopy (AFM). Antimicrobial activities of the synthesized AgNP's have been tested against both bacterial and fungal strains by agar well diffusion method. The biomass-capped AgNP's imparted antimicrobial activity by inhibiting the growth of *Escherichia coli*, *Pseudomonas aeruginosa, Staphylococcus aureus*, *Bacillus cereus, Aspergillus niger* and *Penicillium chrysogenum*. The antioxidant activities of the synthesized AgNP's exhibit low IC_{50} value of ~55.72 µg/mL. Studies on drug loading and kinetics of drug release reveal that *I. tinctoria* AgNP's follow the zero-order kinetics at *p*H 4.6 and *p*H 7.4. The gradient value of 0.568 (*p*H 4.6) and 0.6 (*p*H 7.4) falls between $0.42 < n < 0.85$ when fitted into Peppa's plot indicating that the drug release follow an anomalous transport or non-Fickian diffusion transport, indicating that the diffusion is time dependent.

Keywords: Biological activity, Drug release, *Indigofera tinctoria*, Kinetics, Silver nanoparticles

Indigofera tinctoria Linn, is a leguminous plant, belonging to Fabaceae family, widespread across tropical regions, and has been cultivated for centuries as the main source of indigo dye, giving it a common name "true indigo"[1]. *I. tinctoria* has been reported to be enriched with antitoxic, haemostatic and sedative properties. It is used in the treatment of cancer, piles, chronic bronchitis, asthma, ulcers, gout, rheumatoid arthritis, lumbago, epilepsy, insanity, urinary complaints, cough, rhinitis, palpitation, hepatitis, splenomegaly, hemorrhoids, sores, constipation, leucoderma, grey hairs, snake bite, etc[2-4].

Recently, synthesis of metal nanoparticles from biological sources is gaining significant interest owing to their unique physicochemical properties including optical, catalytic, magnetic, electronic and antimicrobial properties[5]. Particular among them is silver nanoparticles which are reported to play a considerable role in field of medical and biological sciences. They are reported to exhibit high antibacterial, antifungal, anti-inflammatory, antioxidant and antiviral activities, as also playing a crucial role in drug delivery, tissue engineering, gene delivery, artificial implants, diagnosis, imaging and sensing[6].

Earlier studies with reference to this plant indicated that its ethanol extract is effective in reducing the severity of *status epilepticus* and also possesses both *invitro* and *invivo* antioxidant activities[2,3]. The antioxidant activity was said to be directly related to the total amounts of phenolics and flavonoids found in the extract[3,7,8]. Other studies reported that *I. tinctoria* has good antibacterial[9] and antihepatotoxic activities[10]. Two important antibacterial compounds were isolated from the methanol extract and named "indicant" and "sumatrol"[11]. Indigotine, another fractionated compound from *I. tinctoria* petroleum ether extract, also revealed hepato-protective activity[12]. Nevertheless, to the best knowledge of the authors, only one paper is available on the synthesis of silver and gold nanoparticles from *I. tinctoria* and *I. cordifolia* leaves extract which was assessed for its anticancer, antimicrobial, antioxidant and catalytic properties[13,14].

In the present study we investigated the synthesis of stable AgNP's with the bio-reduction method from

the extract of *I. tinctoria* .The optimization of various reaction conditions for nanoparticles synthesis viz., metal ion concentration, *p*H and temperature were carried out. In addition to the characterization, the antimicrobial and antioxidant properties of synthesized AgNP's have as well been explored. Furthermore, for the first time the kinetics of *in vitro* release of Doxorubicin (DOX), a major chemotherapeutic drug, from the drug loaded AgNP's was also studied in order to determine the suitable model describing the dissolution profile (Scheme 1). AgNP's incorporating anticancer agents can overcome resistance to drug action, thus reducing the need of higher doses subsequently reducing the side effects towards normal cells.

Experimental Section

Materials

Silver nitrate ($AgNO_3$), potassium bromide (KBr) and all other chemicals were purchased from Sigma Aldrich, India. All microbiological media were purchased from Hi Media, India. The bacterial cultures of *E. coli* (ATCC-25922), *P. aeruginosa* (ATCC-27853), *S. aureus* (ATCC-33592) and *B. cereus* (ATCC 10876) were procured from Hi Media India, whereas the fungal cultures *A. niger* (281) and *P. chrysogenum* (161) were procured from Microbial Type Culture Collection, IMTECH, Chandigarh, India. *I. tinctoria* plant sample was collected from East Godavari district area, Andhra Pradesh during day time and was taxonomically identified by the Botanical Survey of India, Hyderabad.

Preparation of *I. tinctoria* plant extract and fabrication of AgNP's therefrom

First of all, plant parts were separated and made free of soil, washed thoroughly with distilled water and shade dried. These were further powdered by using hand pulverizer. About 10g of the material was extracted through hot maceration method using double distilled water and stirred at 200 rpm for 24 h. This was then filtered through muslin cloth and subsequently through Whatman no.1 filter paper; the filtrate was stored at 4°C for future use. For the fabrication of AgNP's one mL of the plant extract was

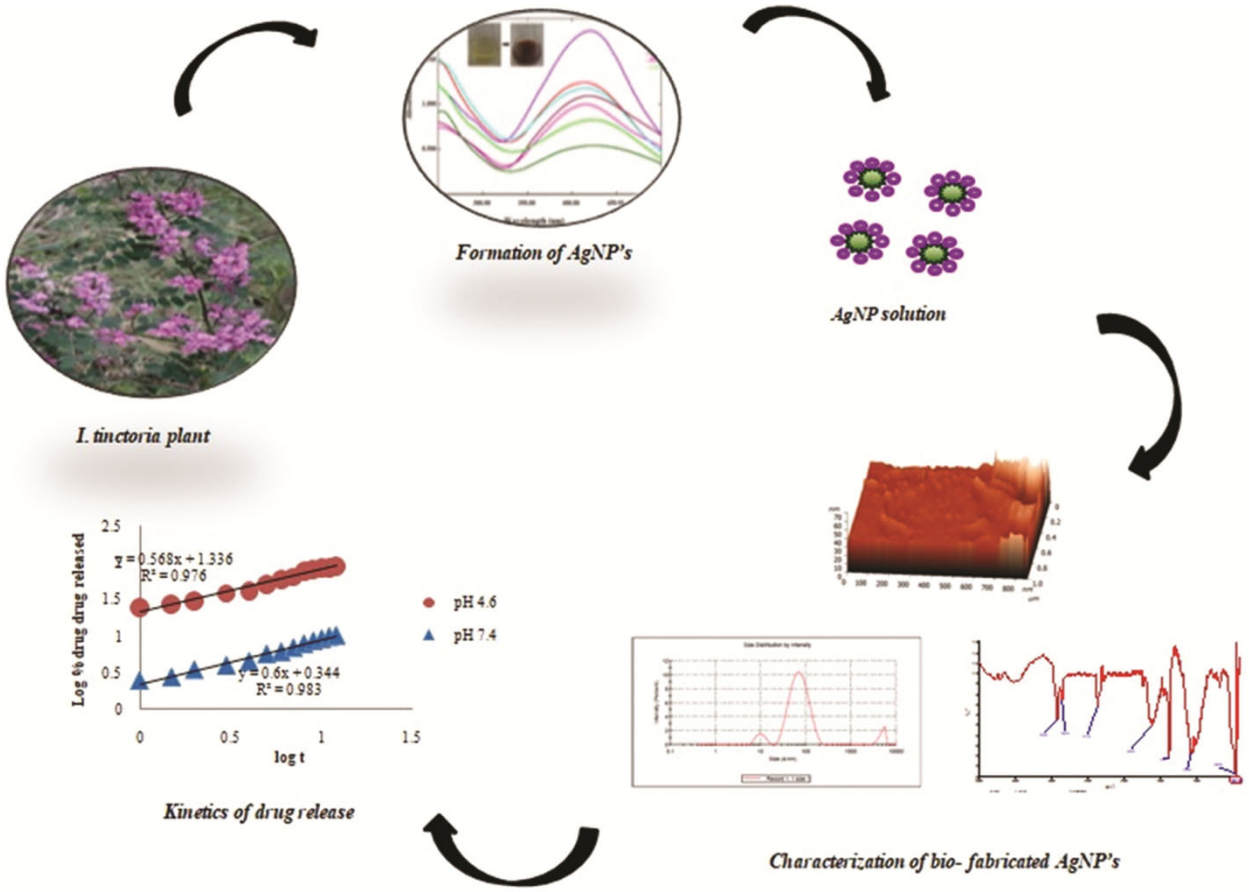

Scheme 1

added dropwise to 10 mL of 1 mM $AgNO_3$ solution and heated. The mixture was incubated in dark condition at room temperature and observed for change in colour if any, at regular intervals and measured for its absorbance by UV-Visible spectrophotometer at 420nm.

Optimization studies

Experiment was performed to assess the formation of nanoparticles when different concentrations of $AgNO_3$ solution (0.5-4.0 mM) were added with plant extract. Further, the influence of plant extract volume and $AgNO_3$ solution were also studied. For this, different volumes of plant extract ranging from 0.25 to 2.0 mL were mixed individually with 10mL of 1mM $AgNO_3$ solution and on the other hand different volumes of $AgNO_3$ solution (5- 45 mL) were mixed with optimized volume of plant extract and observed for colour change which was monitored at 420 nm. Similarly, the influence of *p*H (4.0-12.0) and temperature (25-100°C) on AgNP's formation were also assessed. The nanoparticles synthesized under optimized conditions were centrifuged using ultra-centrifuge (Eppendorf) at 12000rpm for 30min; the obtained pellet was then placed in the -80°C ultra-refrigerator (Biocare) and subjected to lyophilization (Penqu Classic Plus-Lyophilizer) to obtain completely dried nanoparticles for further use.

Characterization of bio-synthesized AgNP's

The optical properties of the AgNP's were analysed by UV-Vis Spectrophotometer (JASCO V760 model) between the wavelengths of 300-600 nm. The FTIR spectra of the control and bio-fabricated AgNP's were recorded in the range of 4000-400 cm^{-1} over 500 scans with a resolution of $2cm^{-1}$. Mean particle size diameter was measured in a solution directly after synthesis. Dynamic light scattering (DLS) and zeta potential measurements were performed using a Malvern Zetasizer (Malvern Instruments, UK). The high-resolution image of the surface of nanoparticles which enrich us with valuable information like size, shape, topography, composition and electrical conductivity and other properties was visualized by SEM-EDX using lyophilized sample of AgNP's. For AFM, a thin film of AgNP's was prepared on the borosilicate glass slide to analyse the surface morphology. The prepared thin film was analysed in the tapping mode using AFM; NT-MDT Integrated Solutions for Nanotechnology.

Evaluation of antioxidant activity of the synthesized AgNP's

The *in vitro* free radical scavenging activity was assessed by using 1, 1-diphenyl-2-picrylhydrazyl (DPPH) reagent[15]. DPPH is a stable free radical which reacts with an antioxidant compound that can donate hydrogen and gets reduced to become a stable diamagnetic molecule. The change in colour from deep violet to light yellow was measured, wherein the intensity of the yellow colour depends on the amount and nature of radical scavenger present. Briefly, reaction mixture containing 1 mL of 0.1 mmol/L DPPH with different concentrations of nanoparticles (20, 40, 60, 80 and 100 µg) were made up to 3 mL using deionized water and further incubated for 10 min. The formed yellow colour chromophore was measured at 517 nm. Butylated hydroxyl toluene (BHT) was used as a standard for comparison.

Antimicrobial activity of synthesized AgNP's

The antimicrobial activity was carried out by agar well diffusion assay[16] using Gram positive, Gram negative bacteria and fungi. Briefly, nutrient agar and potato dextrose agar were prepared and sterilized. Approximately 20 mL of the media was poured in petri plates and cooled. 200 µL of the 16-18 h young cultures of different bacterial strains and fungal spores were spread on the respective media by using L-rod. On each plate 5.0 mm diameter wells were bored using sterile cork borer and added with50and 100 µL of extract (10 mg/mL) and synthesized AgNP's (10 mg/mL) both dissolved in dimethyl sulfoxide (DMSO). Wells filled with 100 µL of Ciprofloxacin/ Nystatin (100 µg/mL) and 100 µL of DMSO served as positive and negative controls, respectively. The bacterial culture plates were incubated at 35 $\pm$ 2°C for 24-48 h and fungal culture plates at 32 $\pm$ 2°C for 48-72 h. Each experiment was performed in triplicate and the values for zone of inhibition were noted after incubation period.

Loading of Doxorubicin (DOX) to AgNP's and in vitro release studies

For loading of drug to synthesized AgNP's, a calculated amount of DOX was added to AgNP's dispersion, resulting in a final DOX concentration of 10^{-4} M (0.1 mg in 2 mL). The mixture was stirred at 1000 rpm for 30 min and further incubated at room temperature for 24h for complete loading of drug onto nanoparticles. After this it was centrifuged at 15000 rpm for 30 min. The obtained pellet was separated from the supernatant and re-dispersed in deionised water prior to further characterization. The

DOX concentration in re-dispersed pellet was determined by measurements of its UV absorbance at 480 nm and the percentage loading of DOX on AgNP's was calculated using thestandard formula.

The *in vitro* drug release studies were carried out at 37 °C at two different *p*H's viz., 4.6 and 7.4 in a glass apparatus. Initially the dialysis tube containing DOX loaded AgNP's (DOX concentration 2 mg) was transferred to a beaker containing 100 mL of phosphate buffer (*p*H 7.4) accompanied with continuous stirring at 100 rpm. The sink condition was maintained by removing 5 mL sample at regular intervals and substituting with equal volume of buffer. The amount of DOX released was analysed using a spectrophotometer at 480 nm. Similar study was undertaken in acetate buffer (*p*H 4.6). These studies were performed in triplicate for each sample[17].

Kinetics of *in vitro* drug release

Various mathematical models have been used to determine the kinetics of drug release from drug delivery systems. When mathematical formulae are used to describe the process, it becomes easier to quantitatively analyse the values obtained in release rates. These models can ultimately help to optimize the design of a therapeutic device to yield information on the efficacy of various release models. In the present study, different equations like zero order[18], first order[19], Higuchi's model[20] and Korsmeyer–Peppas plot[21] were used to used to study the kinetics of *in vitro* drug release.

Results and Discussion

The present investigation demonstrates the green synthesis of AgNP's using plant extract of *I. tinctoria*, after optimizing various parameters. Subsequently, the nanoparticles were characterized using various instrumental techniques followed by elucidating the antioxidant and antimicrobial activities. The nanoparticles were further loaded with DOXand studies for its release kinetics using various mathematical models were carried out.

Identification of plant specimen and synthesis of AgNP's from its extract

The plant used in the current study was taxonomically identified by the experts of Botanical Survey of India, Hyderabad as *I. tinctoria*. The *I. tinctoria* extract before and after addition to the $AgNO_3$ solution (colourless) can be observed in the inset of Fig. 1. The formation of the AgNP's by the reduction of $AgNO_3$ is indicated by change in the color of the plant extract from light yellow to dark brown[22]. The UV–visible absorption spectra of the AgNP's at different time intervals after addition of the *I. tinctoria* extract is depicted in Fig. 1. The absorption peak observed between 410-425 nm known as Surface Plasmon Resonance (SPR) band is generated by the oscillation of conduction electrons in resonance with light wave, which is the characteristic of AgNP's[23]. The maximum absorption intensity is observed at 30 min indicating that the reaction is completed within 30 min after which there is a decrease in peak intensity, attributed to the aggregation of the nanoparticles. This is due to the fact that when particles aggregate, the conduction electrons near each particle surface become delocalized and are shared amongst neighbouring particles leading to decrease in absorption intensity.

UV-visible absorption spectrum can also be used to predict the size of nanoparticles. Smaller AgNP's predominantly absorb light near 400 nm, while larger particles exhibit increased scattering and therefore the absorption peak broadens and the absorption maxima suffers a red-shift towards longer wavelength[24].In the present case, the absorption maxima lie at 419.6 nm (30 min), which is slightly blue shifted to 413.6 nm at 45 min. This indicates that the AgNP's formed at 30 min get stabilized at 45 min and theaverage diameter of the AgNP's estimated from the λ_{max} value is 40-50 nm[23]. Nanoparticle formation depends on the factors such as concentration, incubation time, *p*H and temperature. This study suggests which factor affects the nanoparticles synthesis.

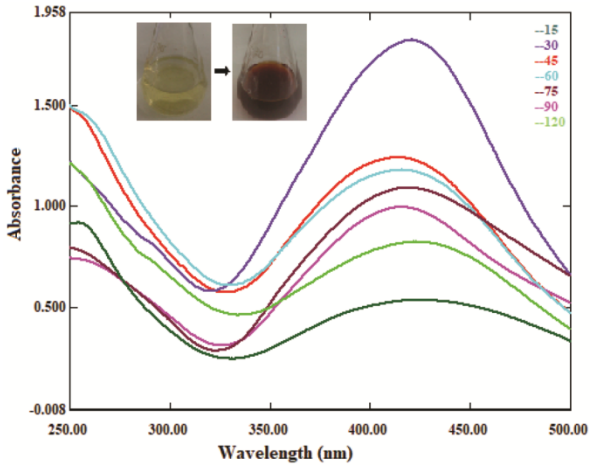

Fig. 1 — Change in color as a result of *Indigofera tinctoria* plant extract due to formation of AgNP's at different time intervals

Optimization of different parameters for AgNP's synthesis

While experimenting using different concentrations of $AgNO_3$ it was observed that the absorption increased along with the increasing concentration of the nanoparticles from 0.5 to 4.0 mM due to higher availability of silver ions for the plant extract (Supporting Information Fig. S1). It was noted that there was a substantial increase in nanoparticles formation when concentration was raised from 0.5 to 1.0mM, which remained more or less constant in subsequent concentrations. Even though other concentrations (2–4 mM) enable the synthesis of AgNP's, 1.0 mM concentration was chosen for further experiments due to their less toxicity as compared to the other concentrations. It is also reported earlier that higher concentration of $AgNO_3$ produces nanoparticles with larger particle size, which may be unstable and show aggregation[25]. The optimization study with respect to different volumes of $AgNO_3$ solution showed a significant effect on the synthesis of AgNP's. Nevertheless, a ratio of 1:10 (*I. tinctoria* extract: $AgNO_3$ solution) yielded the highest amount of nanoparticles (Fig. S2). Conversely, while experimenting with different volumes of plant extract, it was observed that the optimum ratio of plant extracts: $AgNO_3$was found to be 2:10 (Fig. S3). Hence, this ratio was optimized for further studies.

*p*H has a significant role in the synthesis of the AgNP's, the shape and the size of the nanoparticles depend on it. An increase in the absorbance with increase in *p*H suggested that alkaline reaction condition was more appropriate for AgNP's biosynthesis. Nevertheless, an increase in the *p*H from 10.0 to 12.0 decreased the absorbance value with the broadening of the peak. This investigation shows that alkaline *p*H is more suitable for the formation of the AgNP's for this plant extract (Fig. 2).

Temperature is another critical parameter that affects the formation of the nanoparticles. The rise in the formation of nanoparticles is observed with the increase in the reaction temperature using the extracts of *I. tinctoria* (Fig. 2). The absorbance band showed slightly broader peak at low temperature which represents the formation of larger nanoparticles. This experiment suggests that the slow rate of the AgNP's formation can be increased by increasing the temperature of the reaction mixture, which led to fast reduction rate of the Ag^+ and the subsequent nucleation of the silver nuclei allowing the formation of small sized AgNP's. The optimum temperature for the synthesis of AgNP's in the present study was found to be 60°C (Fig. 3). Nevertheless, it is reported that nucleation gets larger with increasing reaction temperature, and it became sensitive to temperature under high-temperature region[26].

Characterization of synthesized AgNP's

FTIR analysis of *I. tinctoria* extract and freeze-dried AgNP's obtained there from to identify the possible interactions between silver and bioactive molecules, which may be responsible for synthesis and stabilization (capping material) of AgNP's was carried out and depicted as Fig. 4.

Both the FTIR spectra were very similar to each other except the strong absorption band at 1385 cm^{-1} in

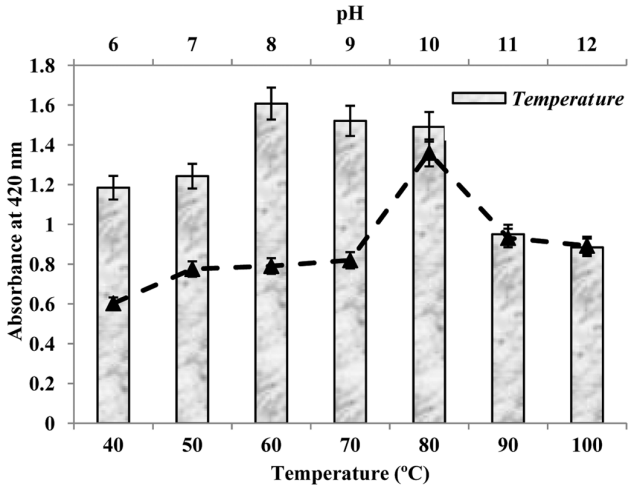

Fig. 2 — Effect of different *p*H and temperature on the formation of AgNP's from *Indigofera tinctoria* extract

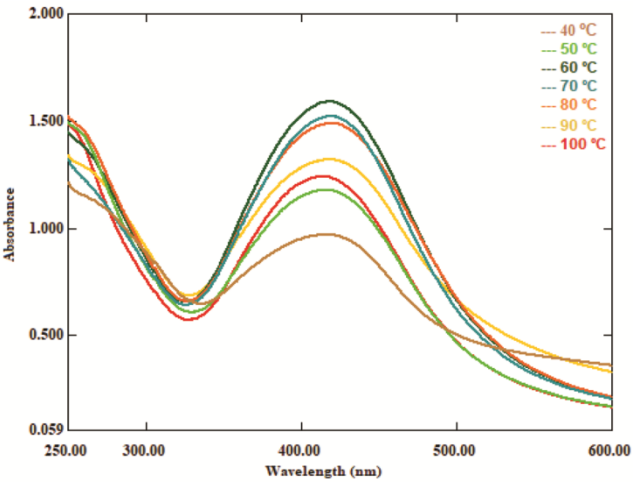

Fig. 3 — UV-Visible spectrum depicting the effect of temperature on synthesis of AGNP's from *Indigofera tinctoria* extract

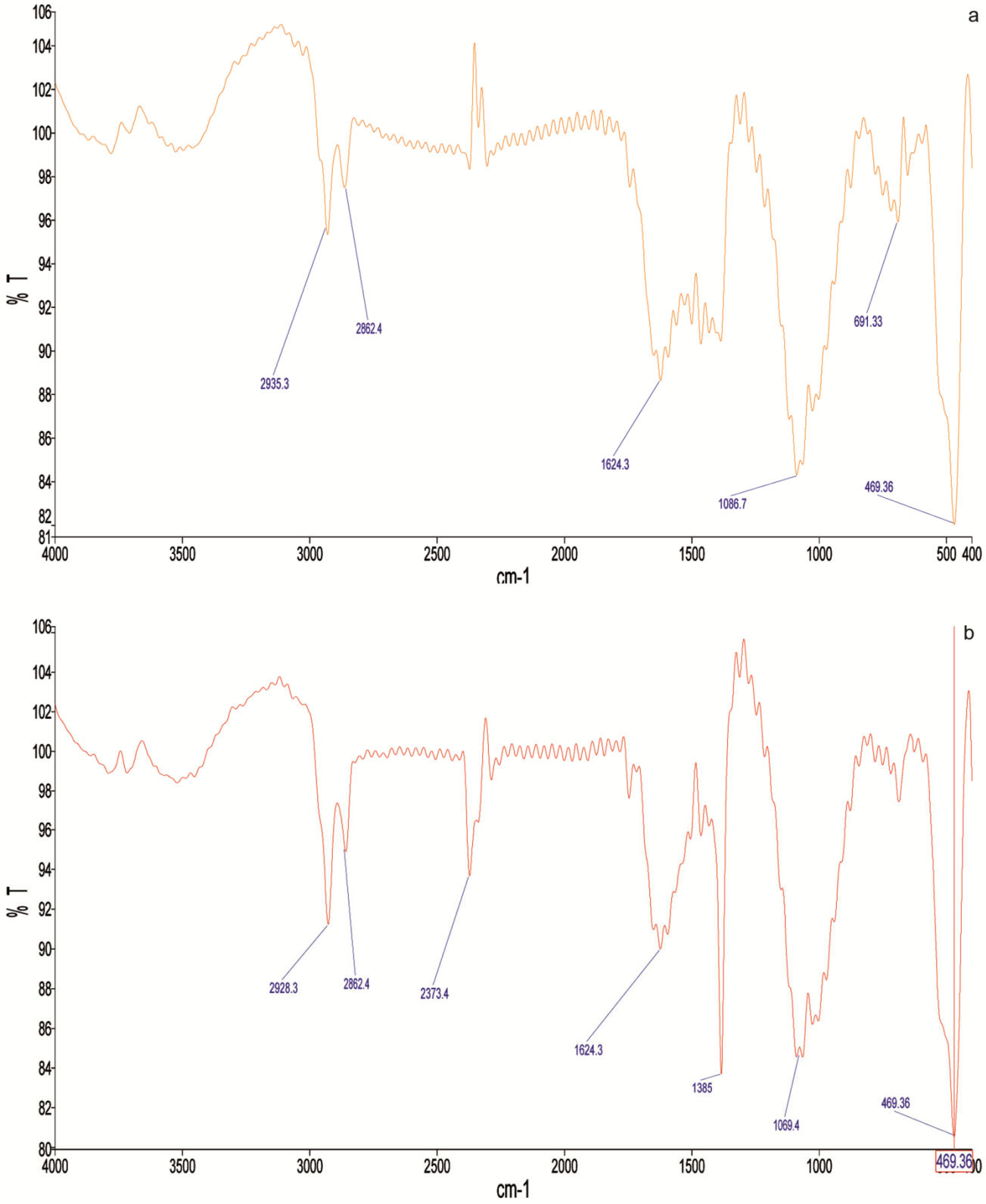

Fig. 4 — FTIR of *Indigofera tinctoria* extract (a) and AgNP'sobtained therefrom (b)

the AgNP's – leaf extract (Fig. 4b), which is due to the anti-symmetric stretching vibrations of the nitrate ions[27]. The high intensity of this peak indicates reasonably high concentration of nitrate ions. Both the spectra show a broad band between 3300 to 3600 cm^{-1}, which can be attributed to the absorption peak due to hydrogen bonded –OH groups of water.The C=O stretching is observed nearly at 1738 cm^{-1}. Symmetric and anti-symmetric stretching vibrations from the aliphatic –C-H group are observed at 2935 and 2862 cm^{-1} (Ref.28). Moreover, the-N-H bending and –C-OH stretching vibrations are observed nearly at1624 and 1086 cm^{-1}, respectively[29]. Shifting of the absorption peak due to –C-OH stretching vibrations from 1086 cm^{-1} (Fig. 4a) in the leaf extract to 1069 cm^{-1} (Fig. 4b) in the AgNP's – extract, indicates interaction of the AgNP's with the –C-OH group of the extract.

The Zeta potential value of the AgNP's synthesized using *I. tinctoria* leaf extract is -17.3 ± 7.8 mV (Fig. 5). The zeta potential value is in the threshold level of delicate dispersion[30] i.e. the aqueous dispersion of the nanoparticles has moderate dispersity. Negative zeta potential value of the AgNP's might be due to adsorption/interaction of OH^- ions, which is also reflected in the FTIR spectrum as shifting of –C-OH absorption band from 1086 to 1069 cm^{-1}. This adsorption/interaction of the nanoparticles with OH^- ions helps in preventing the aggregation through electrostatic repulsion among the negative charges[31].

The average particle diameter obtained by DLS analysis is 62.7 nm in the aqueous colloidal solution (Fig. 5). The particle size distribution shows three peaks at 10.3, 77.7 and 4872 nm, of which the peak at 4872 nm might be due to the agglomerates. Nevertheless, the presence of two peaks at 10.3 and 77.7 nm indicates wide particle size distribution of the synthesized AgNP's. Similar findings on the zeta potential and particle size distribution of AgNP's synthesized from Symphytum of *Cinale* leaf extract has been reported[32].

Figure 6 represents the SEM-EDX image of AgNP's bio-fabricated from *I. tinctoria* leaves extract. AgNP's possessed a spherical structure, in a size range of 10-30 nm.

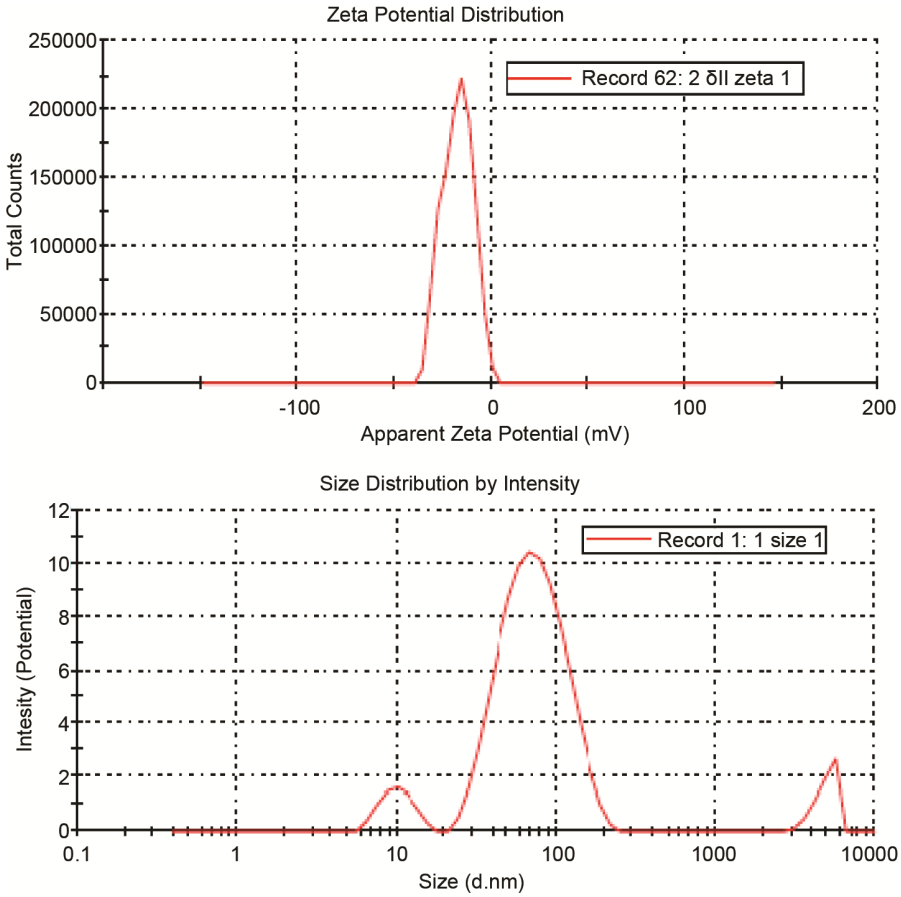

Fig. 5 — Particle size and zeta potential of the AgNP's synthesized from *Indigofera tinctoria* extract

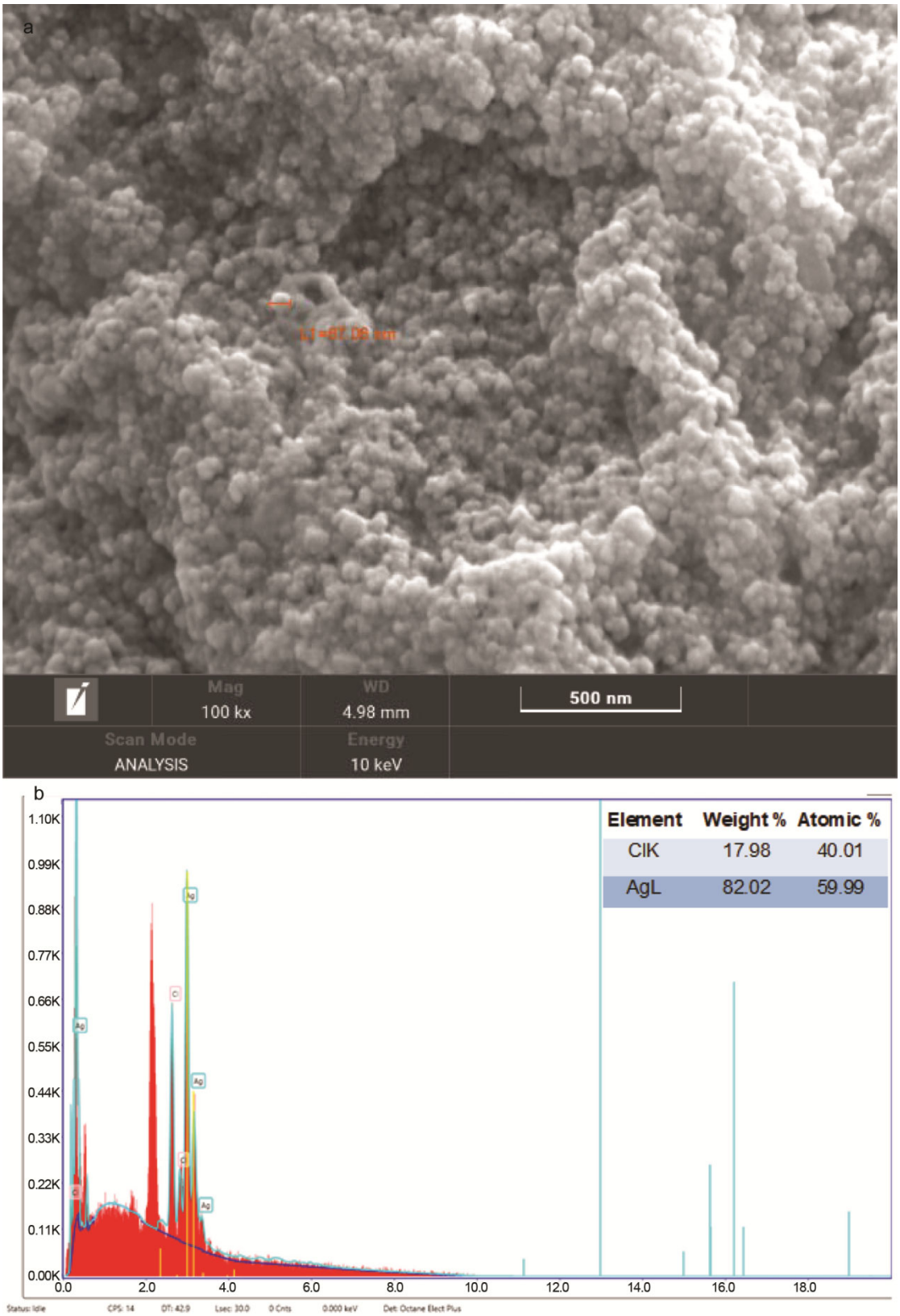

Fig. 6 — SEM micrograph (A) and SEM-EDX (B) of the synthesized AgNP's

Surface topology of the formulated AgNP's was studied by AFM analysis as shown in Fig. 7. The micrographs of the green synthesized AgNP's were obtained with AFM in solid and in semi-contact mode. The micrographs clearly indicated that the formulated AgNP's possess spherical shape and have the calculated sizes below 50 nm.

Pharmacological evaluation

Antioxidant activity

The antioxidant activities of *I. tinctoria* plant extract and synthesized AgNP's were evaluated by DPPH assay using butylated hydroxy toluene as standard (Table 1).

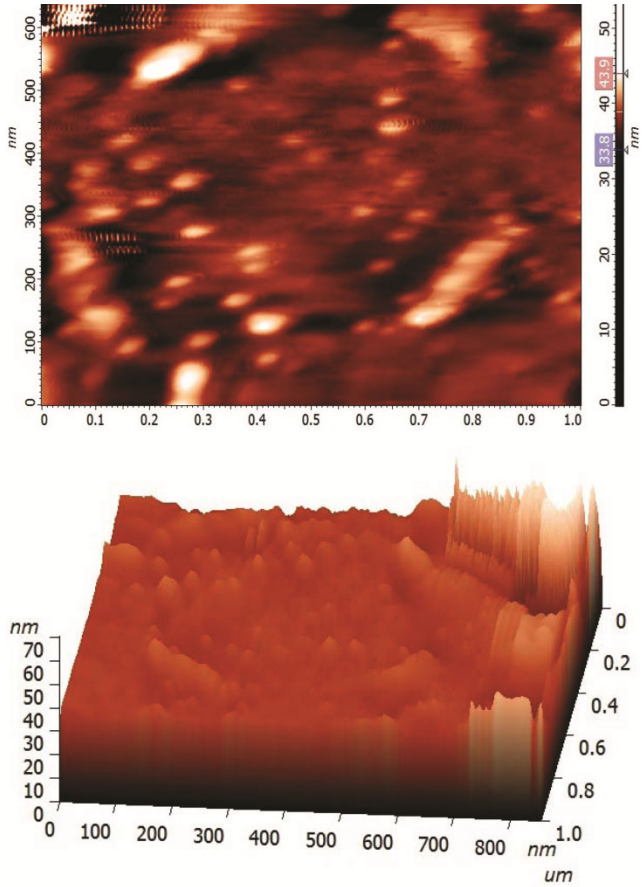

Fig. 7 —AFM showing the AgNP's synthesized from *Indigofera tinctoria* a) 2d image b) 3d image

The DPPH is a stable red coloured, free radical which reacts with antioxidative compounds and gets reduced. Most of the phenolic compounds in the plant extract show high levels of antioxidant activity due to the presence of -OH group[33]. The percent inhibition of synthesized AgNP's was found to be higher than the plant extract as well as standard and increased with increasing concentration of the substrate. The IC_{50} values of the plant extract and AgNP's therefrom was 59.21 and 55.72 µg/ mL respectively. Nevertheless, in another study the IC_{50} values of *I. tinctoria* extract, AgNP's therefrom and AuNP's therefrom were reported to be 177.52 ± 0.43 µg/mL, 10.04 ± 0.51 µg/mL and 68.05 ± 0.71 µg/mL respectively using ascorbic acid as standard[13].

Antimicrobial activity

The antimicrobial activity of plant extract as well as synthesized nanoparticles was carried out by agar well diffusion method. For this, two Gram positive, two Gram negative and two fungal strains were used as mentioned in the material and methods section. The antimicrobial activities of *I. tinctoria* plant extract and AgNP's synthesized there from are shown in Table 2. It was observed that all the six strains exhibited zone of inhibition by plant extract as well as AgNP's synthesized therefrom. Even though antimicrobial activities were exhibited towards all the tested strains, maximum activity was shown toward Gram negative bacteria, which were higher even than the standard. There are several mechanisms proposed for the antimicrobial properties of nanoparticles. The

Table 1 — Antioxidant activity of *I.tinctoria extract and* AgNP's synthesized there from

Concentration (µg)	BHT	*I. tinctoria* extract	*I. tinctoria* nanoparticles
		% inhibition	
20	13.98	14.02	18.66
40	31.11	32.16	35.62
60	48.06	48.16	50.77
80	61.14	60.12	63.39
100	73.31	71.26	75.65
IC_{50}	60.89 µg/mL	59.21 µg/mL	55.72 µg/mL

Table 2 —Antimicrobial activity of AgNP's bio-fabricated using *Indigifera tinctoria* Ramam extract (values in mm)

Treatment / Test organism	Ciprofloxacin/Nystatin(100 µL/well)	*I. tinctoria* extract (50µL/well)	*I. tinctoria* extract (100 µL /well)	*I. tinctoria* AgNP's (50µL/well)	*I. tinctoria* AgNP's (100µL /well)
S. aureus	22.0 ± 0.3	9 ± 0.1	11 ± 0.2	11 ± 0.2	14 ± 0.2
B. subtilis	20.0 ± 0.4	5 ± 0.1	8 ± 0.1	8 ± 0.1	12 ± 0.2
P. aeruginosa	18.0 ± 0.4	11 ± 0.2	14 ± 0.3	18 ± 0.3	20 ± 0.3
E. coli	18.0 ± 0.2	13 ± 0.1	16 ± 0.3	20 ± 0.3	23 ± 0.3
A. niger	23.0 ± 0.1	10 ± 0.3	14 ± 0.2	12 ± 0.1	16 ± 0.2
P. chrysogenum	20.0 ± 0.1	9 ± 0.2	13 ± 0.2	10 ± 0.1	15 ± 0.2

bactericidal activity of AgNP's against broad range of bacteria has been proven in several studies which confirm the multifaceted strategy of AgNP's in the bacteria exposure[34]. The mechanism of bactericidal activity of AgNP's is most likely due to the attachment of the AgNP's to the cell wall. The smaller size and high surface to volume ratio of nanoparticles enables them to interact closely tothe microbial membrane[35]. They disturb the membrane permeability by penetrating in the cell membrane and causing intracellular ATP leakage and cell death[36]. The positively charged Ag^+ ions are known to have a high tendency and affinity to act with phosphorus and sulfur present in biomolecules such as DNA and RNA in the cell membrane, resulting in the disruption of DNA and RNA functions[37]. The Gram positive bacteria are less affected by AgNP'sthan Gram negative bacteria which may be attributed to the presence of large amounts of peptidoglycan layers in the cell walls of Grampositive bacteria. These peptidoglycan layers somewhat prevent the nanoparticles from reaching the cytoplasmic membrane[38].

Loading of DOX to nanoparticles and kinetics of its release data

DOX, a chemotherapeutic drug, was loaded onto the synthesized AgNP's. The percentage loading efficiency of the drug to the nanoparticles was found to be 69.8% at the acidic *p*H and slightly less at alkaline *p*H. In order to measure the release of DOX loaded onto AgNP's *in vitro* and to evaluate their feasibility to target cancer tissue, DOX loaded AgNP's were exposed to acidic (4.6) and physiological (7.4) *p*H conditions at 37°C. The rate and amount of drug released at regular time intervals from the AgNP's at two different *p*H are depicted in Tables 3 and 4. As observed from the tables, acidic *p*H seems to be quite conducive for drug release since 90.33± 1.25% of drug was released at the end of 12 h, nevertheless for physiological *p*H condition at the end of same

Table 3 ─ Release kinetics of the AgNP's synthesized from *Indigofera tinctoria* at *p*H 4.6

Time	% Drug released	% Drug unreleased	Log % Drug unreleased	√time	log t	log % Drug released
0	0	100	2	0		
0.5	11.28	88.72	1.948	0.707	-0.301	1.052
1	24.83	75.17	1.875	1	0	1.394
1.5	27.80	72.14	1.858	1.224	0.176	1.444
2	30.12	69.88	1.844	1.414	0.301	1.478
3	38.41	61.59	1.789	1.732	0.477	1.584
4	42.03	57.97	1.763	2	0.602	1.623
5	50.25	49.75	1.696	2.236	0.698	1.701
6	60.43	39.57	1.597	2.449	0.778	1.781
7	64.18	35.82	1.554	2.645	0.845	1.807
8	76.61	23.39	1.369	2.828	0.903	1.884
9	80.12	19.88	1.298	3	0.954	1.903
10	84.21	15.79	1.198	3.162	1	1.925
11	86.04	13.96	1.144	3.316	1.041	1.934
12	90.30	9.70	0,986	3.464	1.079	1.955

Table 4 ─ Release kinetics of the AgNP's synthesized from *Indigofera tinctoria* at *p*H 7.4

Time	% Drug released	% Drug unreleased	Log % Drug unreleased	√time	log t	log % Drug released
0	0	100	2	0		
0.5	1.68	98.32	1.992	0.707	-0.301	0.225
1	2.47	97.53	1.989	1	0	0.392
1.5	2.76	97.24	1.987	1.224	0.176	0.440
2	3.46	96.54	1.984	1.414	0.301	0.539
3	3.98	96.02	1.982	1.732	0.477	0.599
4	4.49	95.51	1.980	2	0.602	0.652
5	5.68	94.32	1.974	2.236	0.698	0.754
6	6.10	93.90	1.972	2.449	0.778	0.785
7	6.91	93.09	1.968	2.645	0.845	0.839
8	7.82	92.18	1.964	2.828	0.903	0.893
9	8.56	91.44	1.961	3	0.954	0.932
10	9.20	90.80	1.958	3.162	1	0.963
11	9.85	90.15	1.954	3.316	1.041	0.993
12	10.20	89.8	1.953	3.464	1.079	1.008

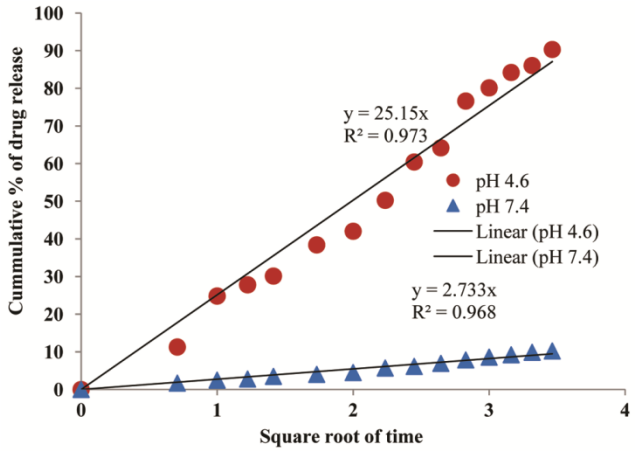

Fig. 8 ─ Zero order plot of drug release kinetics loaded onto AgNP's bio-fabricated from *Indigofera tinctoria* extract at *p*H 4.6 and 7.4

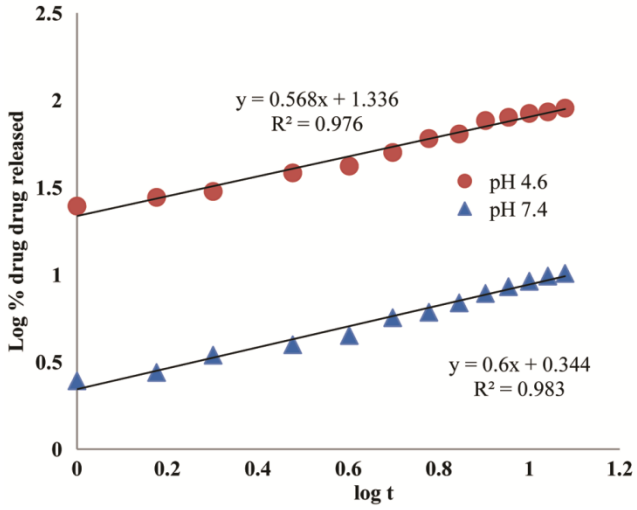

Fig. 9─Higuchi's plot of drug release kinetics loaded onto AgNP's bio-fabricated from *Indigofera tinctoria* extract at *p*H 4.6 and 7.4

time interval the drug release was only 10.2± 1.68%. This type of *p*H dependent release might aid in improving the efficacy of DOX loaded nanoparticles as effective drug delivery systems, where normal cell will not be affected. It is believed that DOX is internalized by cells via endocytosis, wherein the acidic environment of the endosomes may prompt the rapid release of DOX from AgNP's. An additional advantage would be the extreme slow release of DOX in physiological condition which may help to reduce the toxicity of DOX to normal tissues because the *p*H of body fluids is maintained around 7.4[16, 39].

In order to study the kinetics of *in vitro* drug release profile the data was fitted onto various mathematical models. Firstly, the zero-order model was applied to the release profile of drug loaded AgNP's and evaluated (Fig. 8). It refers to the process of constant drug release from a drug delivery system independent of the concentration[40]. The obtained data indicated that drug release from the AgNP's followed the principle of zero order release kinetics due to comparatively higher R^2values (0.983 for *p*H 4.6 and 0.992 for *p*H 7.4). The release experimental data obtained were also fitted into Higuchi model and is presented as Fig. 9. The results indicated the drug release from nanoparticles matrix at both the *p*H showed good fit and followed Higuchi drug release kinetics as evident from high R^2 values (0.973 for *p*H 4.6 and 0.968 for *p*H 7.4). This model is applicable to study the release of water soluble and low soluble drugs incorporated in semisolid and solid matrices[20]. Korsmeyer and Peppas[21] developed an empirical equation to analyse both Fickian and non-Fickian release of drug from swelling as well as non-swelling polymeric delivery systems. In the current study, the diffusion mechanism of the drug release was confirmed by Korsmeyer–Peppas plots with R^2 values 0.976 and 0.983 for *p*H 4.6 and *p*H 7.4 respectively. The gradient value of 0.568 (*p*H 4.6) and 0.6 (*p*H 7.4) (Fig. 9) falls between $0.42 < n < 0.85$, indicating that the drug release followed an anomalous transport or non-Fickian diffusion transport, which means that the diffusion is time dependent.

Conclusion

The current study describes the rapid fabrication of AgNP's using extract of medicinally important plant *I. tinctoria.* Substantial amount of AgNP's were synthesized within 30 min which was confirmed by UV-Vis spectrophotometer. Various process parameters were optimised for enhanced production of AgNP's. The presence of bio molecules in the plant extract as evident by FTIR results suggest their possible rolein thereduction and stabilization of nanoparticles. The average particle diameter obtained by DLS analysis was 62.7 nm in the aqueous colloidal solution. Nanoparticles also exhibited remarkable antimicrobial properties against the selected isolates and antioxidant properties justifying their applications in biomedical field. Further, these nanoparticles loaded with the cytotoxic drug DOX was found to be highlystable without leaching. Efficient uptake of DOX loaded AgNP's at physiological *p*H andresponse at intracellular acidic *p*H makes them an ideal drug delivery system to target cancer cells.

Acknowledgements

The author thanks Director, CSIR-CLRI for support and encouragement.CSIR-CLRI communication number 1459.

Competing interests

The authors declare that there is no competing interest

References

1 Swaminathan C, *Asian J Pharm Clin Res*, 11 (2018) 136.
2 Asuntha G, Prasannaraju Y & Prasad K, *Trop J Pharm Res*, 9 (2010) 149.
3 Anusuya N & Manian S, *Int J Pharm Pharm Sci*, 5 (2013) 142.
4 Srinivasan S, Wankhar W, Rathinasamy S & Rajan R, *J Pharm Anal*, 6 (2016) 125.
5 Ahluwalia V, Elumalai S, Kumar V, Kumar S & Sangwan R, *Microb Pathog*, 114 (2018) 402.
6 Netala V R, Bukke S, Domdi L, Soneya S, Reddy S G, Bethu M S, Kotakdi V S, Saritha K V & Tartte V, *Artif Cells Nanomed Biotechnol*, 46 (2018) 1138.
7 Singh R, Sharma S & Sharma V, *J Integr Med*, 13 (2015) 269.
8 Srinivasan S, Wankhar W, Rathinasamy S & Rajan R, *J Pharm Anal*, 16 (2016)125.
9 Ravichandran R & Alwarsamy A, *Int J Adv Pharm Res*, 3 (2012) 872.
10 Malarvannan L & Devaki T, *J Nat Remedies*, 3 (2003) 49.
11 Sindhu K K & Mathew M M, *J Trop Med Plants*, 13 (2012) 1.
12 Singh B, Saxena A, Chandan B, Bhardwaj V, Gupta V, Suri O & Handa S, *Phytother Res*, 15 (2001) 294.
13 Vijayan R, Joseph S & Mathew B, *Artif Cells Nanomed Biotechnol*, 46 (2017) 861.
14 Siva P K, Sathish M, Parvathi T, Kamraj M, Bhuvaneswari R & Aurmugam M, *J Phytol*, 13 (2021) 48.
15 Brand-Williams W, Cuverlier M E & Berset C, *Lebensmittel-Wissenschaft Technol*, 28 (1995) 25.
16 Perez C, Paul M & Bazerque P, *Acta Biol Med Exp*, 15 (1990) 113.
17 Madhusudhan A, Reddy G B, Venkatesham M, Veerabhadram G, Kumar D A, Natarajan S, Yang M Y, Hu A & Singh S S, *Int J Mol Sci*, 15 (2014) 8216.
18 Hadjiioannou T P, Christian G D, Koupparis M A & Macheras P E, VCH publishers Inc., New York, 1 (1993) 345.
19 Bourne D W A, *Pharmacokinetics*, *Modern Pharmaceutics*, edited by G S Banker & C T Rhodes, 4th Edn, (Marcel Dekker Inc, New York) 2002, 67.
20 Higuchi T, *J Pharm Sci*, 52 (1963) 1145.
21 Korsmeyer R W & Peppas N A, *J Cont Rel*, 1 (1984) 89.
22 Khandel P, Shahi S K, Soni D K, Yadaw R K & Kanwar L, *Nano Convergence*, 5 (2018) 37.
23 Paramelle D, Sadovoy A, Gorelik S, Free P, Hobley J & Fernig D G, *Analyst*, 139 (2014) 4855.
24 Jana J, Ganguly M & Pal T, *RSC Adv*, 6 (2016) 86174.
25 Balashanmugam P, Balakumaran M D, Murugan R, Dhanapal K & Kalaichelvan P T, *Microbiol Res*, 192 (2016) 52.
26 Liu H, Zhang H, Wang J & Wei J, *Arab J Chem*, 13 (2020) 1011.
27 Mandal S, Natarajan S, Suresh S, Chandrasekar R, Jothi G, Muralidharan C & Mandal A B, *Appl Clay Sci*, 115 (2015) 17.
28 Veedu K K, Kalarikkal T P, Jayakumar N & Gopalan N K, *ACS Omega*, 4 (2019) 10176.
29 Nosalova G, Jurecek L, Chatterjee U R, Majee S K, Nosal S & Ray B, *Evid Based Complement Alternat Med*, (2013) 650134.
30 Riddick T M, *Control of colloid stability through zeta potential*, (Wynnewood, Pa) Published for Zeta-Meter, Inc., by Livingston Pub. Co., 1 (1968).
31 Gurunathan S, Kalishwaralal K, Vaidyanathan R, Deepak V, Pandian S R K, Muniyandi J, Hariharan N & Eom S H, *Colloids Surf B Biointerfaces*, 74 (2009) 328.
32 Singh H, Du J, Singh P & Yi T H, *J Nanostructure Chem*, 8 (2018) 359.
33 Orčić D Z, Mimica-Dukić N M, Francišković M M, Petrović S S & Jovin E D, *Chem Cent J*, 5 (2011) 34.
34 Umashankari J, Inbakandan D, Ajithkumar T T & Balasubramanian T, *Aquat Biosyst*, 8 (2012) 1.
35 Morones J R, Elechiguerra J L, Camacho A, Holt K, Kouri J B, Ramirex J T & Yacaman M J, *Nanotechnology*, 16 (2005) 2346.
36 Ajitha B, Reddy Y A K & Reddy P S, *Spectrochim Acta Part A*, 121 (2014) 164.
37 Hajipour M J, Fromm K M, Akbar Ashkarran A, de Aberasturi D J, de Larramendi R, Rojo T, Serpooshan V, Parak W J & Mahmoudi M, *Trends Biotechnol*, 30 (2012) 499.
38 Kawahara K, Tsuruda K, Morishita M & Uchida M, *Dent Mater*, 16 (2000) 452.
39 Aryal S, Grailer J J, Pilla S, Steeber D A & Gong S, *J Mater Chem*, 19 (2009) 7879.
40 Varles C G, Dixon D G & Steiner C, *J Cont Rel*, 34 (1995) 185.